

PROCEEDINGS OF SPIE

SPIDigitalLibrary.org/conference-proceedings-of-spie

Ultrathin tunable terahertz absorbers based on electrostatically actuated metamaterial

Mingkai Liu, Mohamad Susli, Dilusha Silva, Gino Putrino, Hemendra Kala, et al.

Mingkai Liu, Mohamad Susli, Dilusha Silva, Gino Putrino, Hemendra Kala, Shuting Fan, Michael Cole, Lorenzo Faraone, Vincent P. Wallace, Willie J. Padilla, David A. Powell, Ilya V. Shadrivov, Mariusz Martyniuk, "Ultrathin tunable terahertz absorbers based on electrostatically actuated metamaterial," Proc. SPIE 11159, Electro-Optical and Infrared Systems: Technology and Applications XVI, 1115908 (9 October 2019); doi: 10.1117/12.2534282

SPIE.

Event: SPIE Security + Defence, 2019, Strasbourg, France

Ultrathin tunable terahertz absorbers based on electrostatically actuated metamaterial

Mingkai Liu^a, Mohamad Susli^b, Dilusha Silva^b, Gino Putrino^b, Hemendra Kala^b, Shuting Fan^c, Michael Cole^a, Lorenzo Faraone^b, Vincent P. Wallace^c, Willie J. Padilla^d, David A. Powell^a, Ilya V. Shadrivov^a, and Mariusz Martyniuk^b

^aNonlinear Physics Centre, Research School of Physics and Engineering, Australian National University, Canberra, ACT 2601, Australia

^bSchool of Electrical, Electronic and Computer Engineering, The University of Western Australia, Crawley, WA 6009, Australia

^cSchool of Physics, The University of Western Australia, Crawley, WA 6009, Australia

^dDepartment of Electrical and Computer Engineering, Duke University, Durham, NC 27708, USA

ABSTRACT

High performance tunable absorbers for terahertz (THz) frequencies will be crucial in advancing applications such as single-pixel imaging and spectroscopy. Metamaterials provide many new possibilities for manipulating electromagnetic waves at the subwavelength scale. Due to the limited response of natural materials to terahertz radiation, metamaterials in this frequency band are of particular interest.

The realization of a high-performance tunable (THz) absorber based on microelectromechanical system (MEMS) is challenging, primarily due to the severe mismatch between the actuation range of most MEMS (on the order of 1-10 microns) and THz wavelengths on the order of 100-1000 microns. Based on a metamaterial design that has an electromagnetic response that is extremely position sensitive, we combine meta-atoms with suspended flat membranes that can be driven electrostatically. This is demonstrated by using near-field coupling of the meta-atoms to create a substantial change in the resonant frequency.

The devices created in this manner are among the best-performing tunable THz absorbers demonstrated to date, with an ultrathin device thickness (1/50 of the working wavelength), absorption varying between 60% and 80% in the initial state when the membranes remain suspended, and with a fast switching speed (27 ns). In the snap-down state, the resonance shifts by $\gamma > 200\%$ of the linewidth (14% of the initial resonance frequency), and the absorption modulation measured at the initial resonance can reach 65%.

Keywords: THz, metamaterials, MEMS

1. INTRODUCTION

When designed correctly, metamaterials can act as subwavelength antenna. Recent advances in metamaterials have allowed the design of subwavelength antennae that have unit cells around 2,000 times less than λ (where λ is the wavelength of resonance).¹ This is of great value to miniaturisation technologies such as microelectromechanical systems (MEMS), as it allows the manipulation of wavelengths that would otherwise be inaccessible to MEMS devices fabricated by thin film techniques.

Terahertz (THz) radiation has interesting potential applications in the fields of security, medical and scientific imaging, communications, and quality control/process monitoring.^{2,3} However, the take-up of the use of THz technology for these applications has been slow, due mainly to the exotic materials and complex manufacturing techniques imparting high cost to THz devices.

Further author information: (Send correspondence to G. Putrino)

G. Putrino: E-mail: gino.putrino@uwa.edu.au, Telephone: +618 6488 2559

THz wavelengths range from 0.1 mm to 1 mm (0.1 to 30 THz), and have a limited response to natural materials, and so the manipulation of THz wavelengths by metamaterials techniques is a particularly active field of research.^{4,5} Tunable absorbers for this wavelength range are extremely important for a wide range of applications.⁶⁻⁹ When analysing the effectiveness of tunable absorbers, important figures of merit are that of modulation index, modulation speed, modulation contrast and strength of absorption.

In this work, we combine MEMS and metamaterials techniques to design, fabricate and demonstrate the operation of ultra-thin ($\sim \lambda/50$) tunable THz absorbers. Using thin film deposition techniques, we create suspended silicon nitride membranes that can be electrostatically actuated, and then deposit meta-atoms which support strongly localized modes on these membranes. These devices show excellent performance, demonstrating up to 80% absorption, giant mechanical sensitivity of $\delta\lambda_0/\delta d$ up to 14.8), large modulation contrast of up to 65% change in absorption, and fast switching times of $\sim 27\mu\text{s}$.

2. DEVICE CONCEPT AND MODELLING

The complete device is made up of MEMS movable silicon nitride membranes supporting arrays of meta-atoms. Figure 1(a) shows an isometric image of a single unit cell of meta-atoms. The cell consists of a 200 nm thick ground plane, a 2 μm thick silicon nitride spacer, and a 200 nm thick silicon nitride membrane holding an array of gold meta-atoms suspended an adjustable distance d above the spacer. Each unit cell has dimensions of 180 $\mu\text{m} \times 180 \mu\text{m}$ and consists of nine meta-atoms suspended on the 140 $\mu\text{m} \times 140 \mu\text{m}$ silicon nitride membrane. The membrane is tethered to mechanical beams on all four sides, which can be charged via electrodes to create and electrostatic attraction to the ground plane and so used to actuate the membrane. As fabricated, the separation between the membrane and the spacer is $d = 3 \mu\text{m}$.

The geometry chosen for the individual meta-atoms is based on electric split-ring resonators (ESRRs), as they have been shown to achieve a lower radiative loss and higher quality factor compared to dipole style meta-atoms such as cut-wires and I-beams.¹⁰ The THz response of the ESRR meta-atoms used for this study were simulated with CST Microwave Studio. This software was used to simulate a periodic array of absorbers, where the conductivity of gold was chosen to be $4.56 \times 10^7 \text{ Sm}^{-1}$.

For this study, two types of ESRRs were designed, which have been denoted as “1” and “2”, according to the number of gaps in the meta-atoms. Each design has an additional modifier, which is the two types of membrane geometries used - “S” and “D” denote square and diamond geometries of the membranes, respectively. Figure 2 illustrates the designs for meta-atoms S1, S2, D1, and D2.

Figure 1(c) shows the simulated absorption spectra for meta-atom design S2 for separations $d = 0 - 3\mu\text{m}$ in the window of the THz regime from 0.6-1.2 THz. When the membrane is not actuated ($d = 3 \mu\text{m}$), the resonant frequency is 1.16 THz, and provides absorption of $> 99\%$. The total device thickness is 5.6 μm when measured from the ground plane to the meta-atom layer, therefore the free space wavelength being absorbed is approximately 46 times the device thickness, making this a substantially sub-wavelength device. Figure 1(d) shows the simulated electric field distribution in the device, and it can be seen that the electric field is strongly localized within the gaps of the meta-atoms and enhanced by a factor of > 4000 . These simulations also show that 98.5% of the energy is dissipated in the metal of the meta-atoms. The full width half maximum of the simulated THz resonance was 47 GHz, supplying a Q-factor of 24. The simulations predict that when the membrane is actuated downwards by 1 μm to $d = 2 \mu\text{m}$, the resonance shifts by 40 GHz. At this point, the peak absorption at the new resonance is predicted to be approximately 90%, and a substantial lowering of absorption to 20% is observed for the original resonance frequency of 1.16 THz. When the membrane is driven to $d = 0 \mu\text{m}$, the resonance is predicted to shift by more than 580 GHz, and as seen in Figure 1(c), the absorption at the original resonance frequency of 1.16 THz is extremely close to 0%, providing near perfect absorption modulation.

3. DEVICE FABRICATION

The tunable metamaterial absorbers were fabricated on two-inch silicon wafers using standard surface micro-machining techniques.¹¹ The THz domain spectral measurements of these devices were to be obtained with a commercial THz time-domain spectrometer - specifically, a Terapulse 4000, supplied by Teraview Ltd, UK. Due

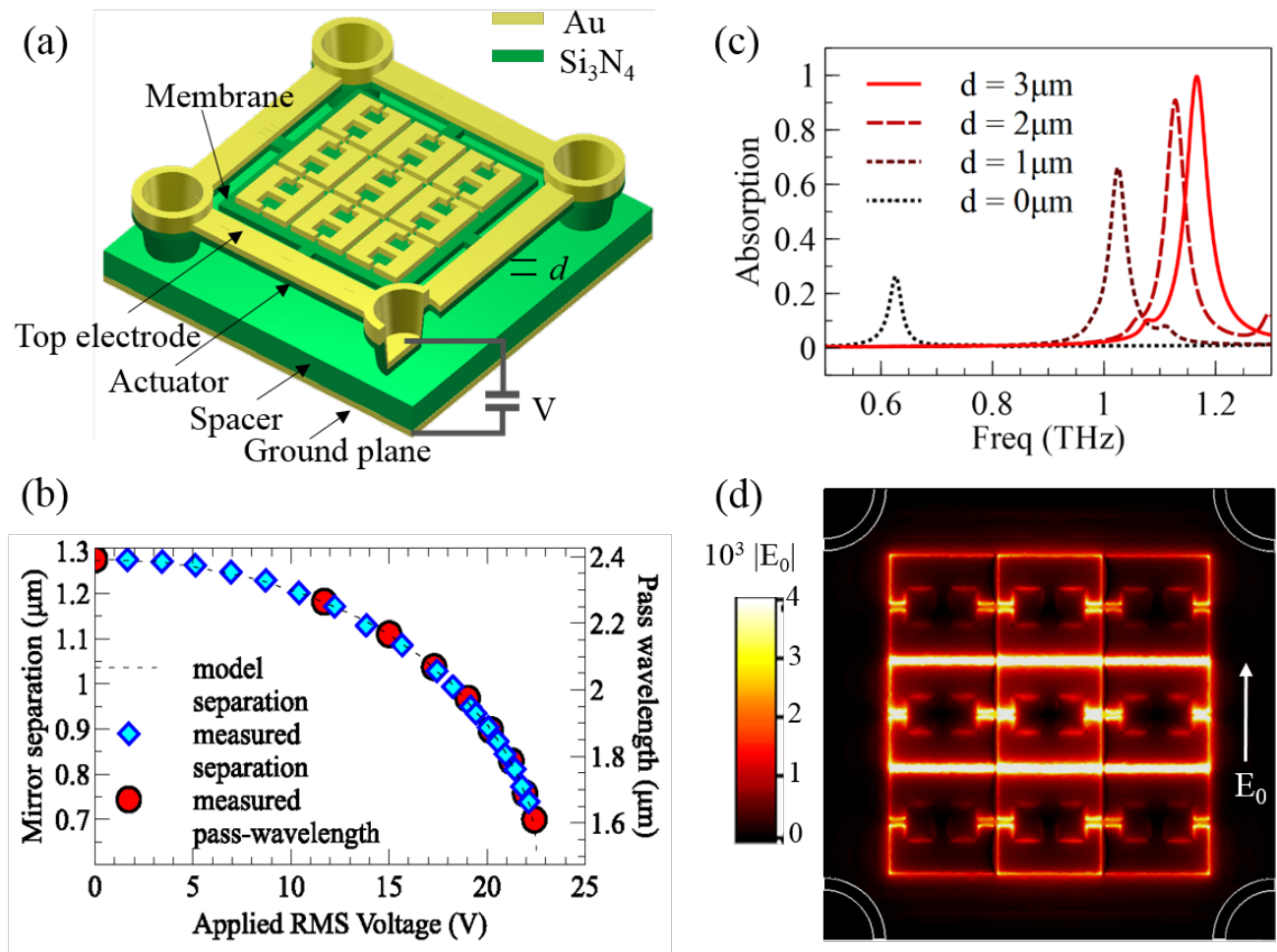


Figure 1. (a) Isometric diagram of a typical unit cell of the THz absorber. Note that the vertical distance d between the meta-atoms and the ground plane can be tuned electrostatically, and that various meta-atom designs other than that pictured here were trialed. (b) Measured actuation distance - voltage curve for one of the fabricated MEMS devices. (c) Electromagnetic simulations of absorption spectra over the range $d = 0 - 3\mu\text{m}$. (d) Amplitude of the electric field in the plane of the meta-atoms at the absorbing THz wavelength, normalized to the incident electric field amplitude $|E_0|$

to the spot size of the characterization beam emitted by this device, unit cell arrays of two sizes - $5\text{ mm} \times 5\text{ mm}$ and $10\text{ mm} \times 10\text{ mm}$ - for each absorber design were fabricated.

Starting with the two-inch silicon wafer, first a gold ground plane was created using electron-beam (e-beam) deposition. Following this, the $2\mu\text{m}$ silicon nitride spacer layer was deposited using inductively coupled plasma chemical vapor deposition (ICPCVD). Gold wiring electrodes were then deposited via e-beam, then patterned using a lift-off process. At this point, the wafer was spin-coated with a polyimide sacrificial layer. This sacrificial layer was patterned to create anchor holes using photolithography and wet etching techniques. The structural layer of the device, being the posts, beams and support membranes were deposited via ICPCVD, then patterned using reactive ion etching (RIE). The meta-atoms were then deposited via e-beam and patterned with a lift-off process. Finally, the polyimide sacrificial layer was removed using an oxygen plasma ash, which released the suspended structures.

The optical resonance of these devices is very sensitive to the distance between the ground plane and meta-atoms, therefore bowing of the membrane negatively effects device performance. It is important to achieve optimal flatness in the top membrane carrying the meta-atoms. Through the deposition of an additional thin layer

of silicon nitride with controllable in-built stress directly underneath the gold meta-atom, the undesired stress is compensated in a controllable fashion. Maximum bowing of 100 nm was achieved over the $140\text{ }\mu\text{m}\times 140\text{ }\mu\text{m}$ suspended membrane area. Without this stress compensation layer, membrane bowing leads to significant resonance broadening and potential splitting.

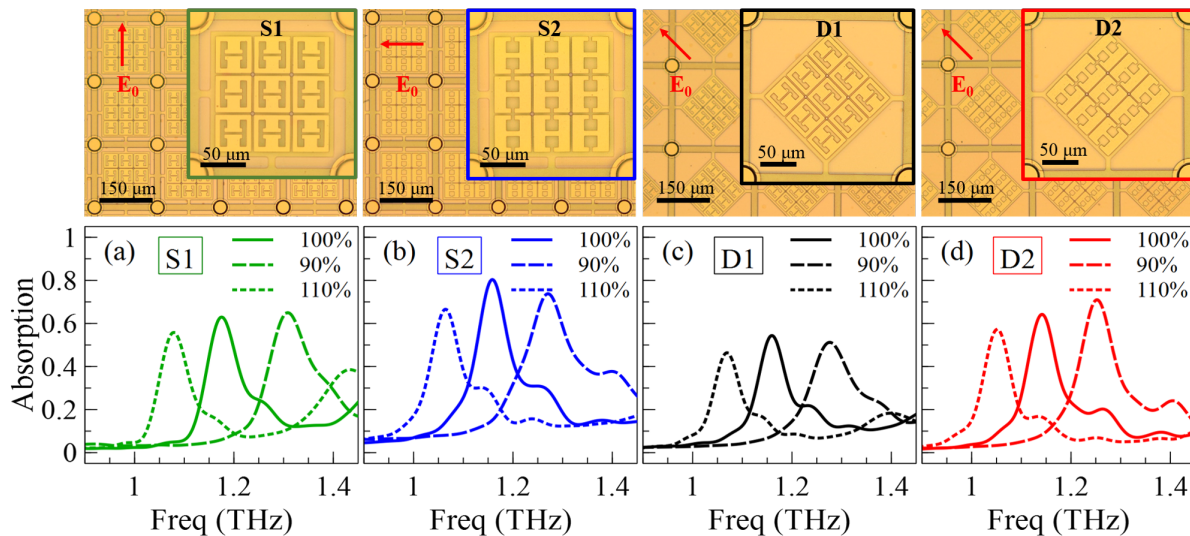


Figure 2. Optical microscope images and the measured THz absorption spectra of fabricated MEMS filters. Two ESRR designs (designated “1” and “2”), with two membrane designs (“S” and “D” denoting square and diamond respectively). Devices with geometry scaled by 90% and 110% have also been fabricated, and their spectra measured. Red arrows indicate the polarisation of the incident electric field during measurement.

4. RESULTS AND DISCUSSION

Reflection spectra was measured using a commercial THz time-domain spectrometer (Terapulse 4000, Teraview Ltd, Cambridge UK). Results were verified using a second commercial THz time-domain spectrometer (EKSPLA, Vilnius Lithuania). All samples were measured in a chamber purged with nitrogen in order to remove atmospheric effects such as humidity. The measured absorption for each of the four designs when the devices are at rest are shown in Figure 2. These measurements show that design “2” provides strongest absorption. The highest absorption of 80% was observed in sample S2. It can be seen that the diamond lattice implementation of design “2” (device D2) shows a smaller resonance red-shift and a lower absorption. This is due to the reduced fill factor of the meta-atoms in the diamond lattice device design. The fabricated devices at 90% and 110% of the designed meta-atom size show that the optical resonances shifted by approximately $\pm 10\%$, as expected.

The main goal of this investigation was to demonstrate electronically controlled tunability of the absorber. The free-standing membranes carrying the meta-atoms were actuated using electrostatic attraction between the ground plane of the device and the actuation pads on the suspended beam of the device. To perform actuation without causing unwanted charging effects, we employed a periodic square wave voltage alternating between negative and positive with a carrier frequency $f_C = 50\text{ kHz}$. These positive and negative voltages of the same magnitude keep a constant actuation force on the top layer, as electrostatic force is proportional to the square of voltage. THz reflection spectra of the device was measured for various peak-to-peak voltages V_{pp} in the range from 0 to 250 V. This modulation technique is suitable for MEMS membranes of this type as long as the carrier frequency is much higher than any mechanical resonances.

Figure 3 shows the THz absorption characteristics for the samples S1, S2 & S3. Large resonance shifts of approximately 45 GHz for S1 and S2, and approximately 30 GHz for D2 can be seen as the membranes approach the threshold of snap-down. To test maximum modulation, device D2 was driven to snap-down. At snap-down, the resonance shifted by 165 GHz, which is 14.4% of the initial resonance wavelength.

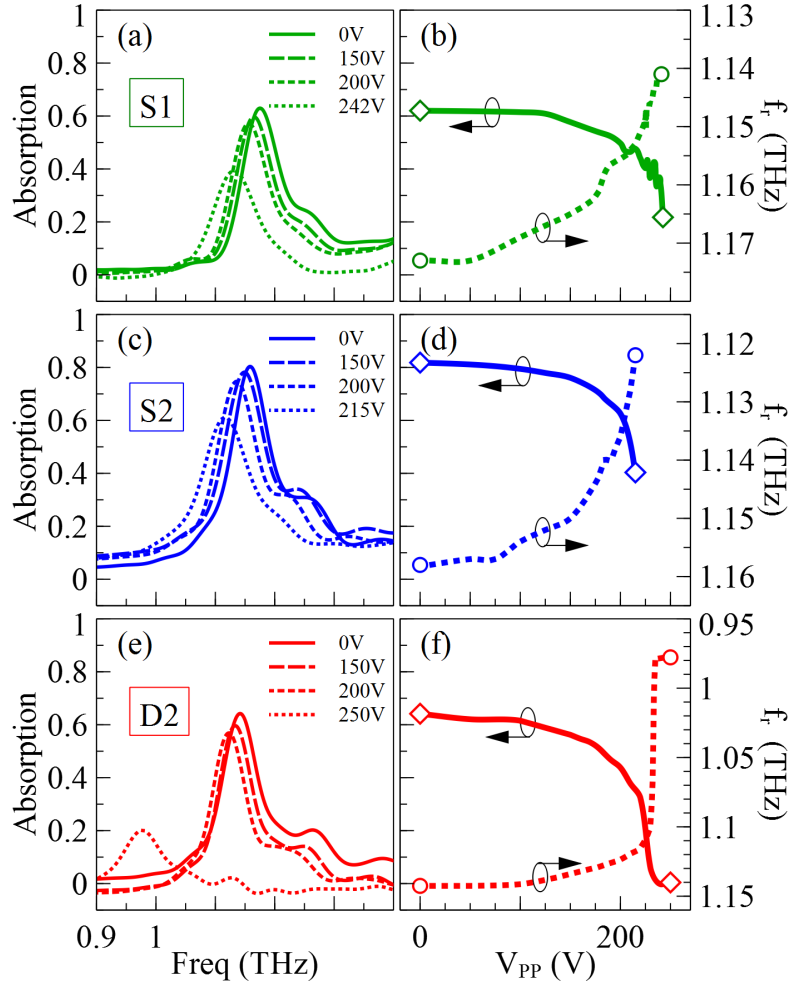


Figure 3. (a), (c) and (e) Measured absorption spectra for different applied peak-to-peak voltages V_{pp} . (b), (d) and (f) show the corresponding absorption change measured at the initial (at rest) optical resonant frequencies of maximum absorption, and also the shift in resonant frequency as voltage actuation increases.

The mechanical response of membrane design S1 when under actuation was monitored using a laser Doppler vibrometer to measure displacement when a voltage signal was applied. Figure 4(a) shows the displacement of the membrane when driven using a 1 kHz square wave (0 to 100 V). This data shows that the device is over-damped at room temperature and pressure (RTP). The 10 to 90% displacement response time was observed to be approximately 27 μ s.

The second mechanical response experiment was performed by applying a voltage with a square wave carrier frequency of 50 kHz that was then modulated with a frequency of 10 kHz. The results of this measurement is shown in Figure 4(b), and it can be seen that the displacement amplitude follows the modulation signal in a repeatable manner. The maximum displacement seen here is less than the displacement observed at 1 kHz in Figure 4(a) due to roll-off of the mechanical response.

The final mechanical test investigated the displacement amplitude as a factor of modulation frequency and is presented in Figure 4(c). As can be seen, the 3 dB high frequency roll-off occurs at approximately 16.5 kHz.

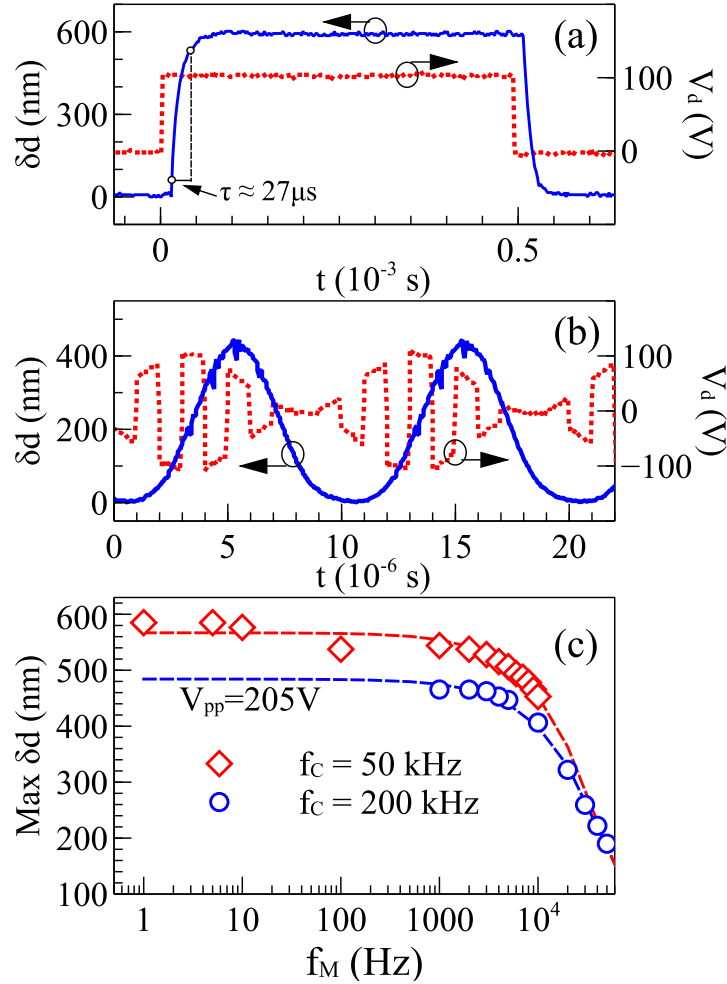


Figure 4. Mechanical response of device S1. V_d is the driving voltage, f_C the carrier frequency, f_M the modulation frequency and δd is the displacement of the membrane. (a) $f_C = 1$ kHz, $f_M = 0$ kHz; (b) $f_C = 50$ kHz, $f_M = 10$ kHz; (c) Maximum displacement for carrier frequencies at (i) 50 kHz and (ii) 200 kHz as a function of modulation frequency. Points depict actual measurements. Dashed curves depict a fit to the measurement data using an exponential decay model.

5. CONCLUSION

This work presented a study of a novel design of an ultra-thin tunable THz absorbers based on MEMS-driven meta-atoms. The device thickness of approximately 1/50 of the working wavelength, absorption varying between 60% and 80% in the initial state and fast switching speed of ($27 \mu\text{s}$), as well as the tuning range of up to 14% of the initial resonance frequency make these among the best performing tunable THz absorbers demonstrated to date. This demonstrated approach could be implemented at low cost, using standard surface-micromachining techniques, and could benefit numerous applications in THz technology.

ACKNOWLEDGMENTS

We acknowledge the support from the Australian Research Council, Western Australian Node of the Australian National Fabrication Facility, and the Office of Science of the West Australian State Government.

REFERENCES

- [1] Chen, W.-C., Bingham, C. M., Mak, K. M., Caira, N. W., and Padilla, W. J., "Extremely subwavelength planar magnetic metamaterials," *Physical Review B* **85**, 201104 (May 2012).

- [2] Malhotra, I., Jha, K. R., and Singh, G., "Terahertz antenna technology for imaging applications: a technical review," *International Journal of Microwave and Wireless Technologies* **10**, 271–290 (Apr. 2018).
- [3] Mathanker, S. K., Weckler, P. R., and Wang, N., "Terahertz (THz) applications in food and agriculture: A review," *Transactions of the ASABE* **56**(3), 1213–1226 (2013).
- [4] Zheludev, N. I. and Kivshar, Y. S., "From metamaterials to metadevices," *Nature Materials* **11**, 917–924 (Nov. 2012).
- [5] Fan, K. and Padilla, W. J., "Dynamic electromagnetic metamaterials," *Materials Today* **18**, 39–50 (Jan. 2015).
- [6] Tao, H., Strikwerda, A. C., Fan, K., Padilla, W. J., Zhang, X., and Averitt, R. D., "Reconfigurable Terahertz Metamaterials," *Physical Review Letters* **103**, 147401 (Oct. 2009).
- [7] Zhu, W. M., Liu, A. Q., Zhang, X. M., Tsai, D. P., Bourouina, T., Teng, J. H., Zhang, X. H., Guo, H. C., Tanoto, H., Mei, T., Lo, G. Q., and Kwong, D. L., "Switchable Magnetic Metamaterials Using Micromachining Processes," *Advanced Materials* **23**(15), 1792–1796 (2011).
- [8] Fu, Y. H., Liu, A. Q., Zhu, W. M., Zhang, X. M., Tsai, D. P., Zhang, J. B., Mei, T., Tao, J. F., Guo, H. C., Zhang, X. H., Teng, J. H., Zheludev, N. I., Lo, G. Q., and Kwong, D. L., "A Micromachined Reconfigurable Metamaterial via Reconfiguration of Asymmetric Split-Ring Resonators," *Advanced Functional Materials* **21**(18), 3589–3594 (2011).
- [9] Kan, T., Isozaki, A., Kanda, N., Nemoto, N., Konishi, K., Kuwata-Gonokami, M., Matsumoto, K., and Shimoyama, I., "Spiral metamaterial for active tuning of optical activity," *Applied Physics Letters* **102**, 221906 (June 2013).
- [10] Liu, M., Fan, K., Padilla, W., Powell, D. A., Zhang, X., and Shadrivov, I. V., "Tunable Meta-Liquid Crystals," *Advanced Materials* **28**(8), 1553–1558 (2016).
- [11] Martyniuk, M., Antoszewski, J., Musca, C. A., Dell, J. M., and Faraone, L., "Stress in low-temperature plasma enhanced chemical vapour deposited silicon nitride thin films," *Smart Materials and Structures* **15**, S29–S38 (Feb. 2006). 00033.